iJRASET
International Journal For Research in Applied Science and Engineering Technology

INTERNATIONAL JOURNAL FOR RESEARCH

IN APPLIED SCIENCE & ENGINEERING TECHNOLOGY

Volume: 5 **Issue:** VII **Month of publication:** July 2017

DOI:

www.ijraset.com

Call: 08813907089 | E-mail ID: ijraset@gmail.com

International Journal for Research in Applied Science & Engineering Technology (IJRASET)
ISSN: 2321-9653; IC Value: 45.98; SJ Impact Factor:6.887
Volume 5 Issue VII, July 2017- Available at www.ijraset.com

Performace Evaluation By Exergy Analysis and Optimization of Organic Rankine Cycle (ORC) by Using Low-Grade Waste Heat

Harwinder Singh[1], R. S. Mishra[2]
[1,2] *Department of mechanical, industrial and production, automobile engineering,*
Delhi Technological University, Bawana road, New Delhi-110042

Abstract: ***This research study deals with the performance evaluation of low-grade exhaust waste heat using organic Rankine cycle (ORC) based on exergy and energy method. Performance variations in ORC system can be analyzed by altering the working parameter settings of the power cycle like the temperature of exhaust gasses or waste heat, evaporator pressure and mass flow rate are considered as independent variables. Performance parameters like exergy and thermal efficiency, net work output and evaporator exergy efficiency are also studied. Organic working fluids for the cycle is R134a, R123, R152a, and R227ea lies between the critical temperature limit of 101.1℃ to 214.1℃. Moreover, performance optimization for organic Rankine cycle is also studied with the help of response surface methodology (RSM) technique with three levels -1, 0 and +1, respectively. Independent variables considered to be optimized with the use of Design Expert software. The Simulation results of exergy efficiency, thermal efficiency and work output of ORC are considered as response variables, and these are concluded by EES software according to the randomly performed 17 treatments of Bob-Behnken design matrix. The responses are fitted into a quadratic polynomial representation and optimizations of these variables are performed simultaneously by using the desirability function (DF) method. At the optimized conditions with a desirability function of 0.990, the optimum value of exergy efficiency, thermal efficiency and work output for R134a are 85.58%, 29.44% and 75.89kJ, respectively.***

Keywords: organic Rankine cycle (ORC), recovery of waste exhaust heat, organic fluids, exergy performance, response surface methodology (RSM), desirability function approach

Nomenclature

$\dot{m}$	mass flow rate (kg/s)
C_P	specific heat (kJ/kgK)
T	temperature (K)
$\dot{W}$	work output (kJ)
S	entropy (kJ/kgK)
$\dot{Q}$	heat rate (kW)
Ex_{inl}	inlet exergy (kW)
$ex_{destruction}$	rate of exergy destruction (kW)
ex	rate of exergy flow (kW)
ORC	organic Rankine cycle
RSM	response surface methodology
h	specific enthalpy
s	specific entropy
X	independent variable
Y	response variable
Z	coded variable
ANNOVA	pareto analysis of variance
e	random error of model
W_{net}	net work output (kJ)

Greek letters

η	efficiency (%)

ISSN: 2321-9653; IC Value: 45.98; SJ Impact Factor:6.887
Volume 5 Issue VII, July 2017- Available at www.ijraset.com

β constant term coefficients of model

I. INTRODUCTION

The Largest amount of waste heat produced in many different types of industrial and commercial applications, which can be efficiently used to generate the power. During the chemical reactions and power plant operation, fuel combustion takes place, in which accountable heat loss produces to the environment is known by waste heat. Therefore, to extract waste heat from the various sources, efficient waste heat recovery methods are employed. In the recent years, attention has been made in the use of ORC system for the heat recovery applications [1-2]. The main difference between the ORC system and the conventional Rankine cycle is that the organic fluid used in ORC. The ORC is a promising and prominent technology, which is commercially feasible to biomass and geothermal power plants [1]. It has been investigated in the previous research that the ORC has a potential to recover the waste heat from the small as well as large-scale engines [3-6]. The selection of working fluids significantly affects to the performance of ORC so that working fluids based on the shape of the vapor saturation curve on a T-S diagram can be divided into three types: dry, isentropic and wet fluids [7, 8]. In addition, thermophysical properties of the fluid, compatibility with materials, safety, and stability at high temperature, environmental impacts and cost are also important parameters to select the optimum fluid [9].

There is a lot of research is available related to analysis and investigation of the ORC performance. Mago [10] investigated the effect of the waste exhaust heat temperature, the pressure of the evaporator, the critical temperature of fluid and temperature difference between pinch point temperature differences (PPTD) based on the exergy analysis of medium grade exhaust waste heat using organic Rankine cycle (ORC). He found that to achieve the smaller PPTD and higher exergetic performance; there should be a marginal dissimilarity between the critical temperature as well as exhaust temperature. Wei et al. [11] conducted a simulation and experimental study related to low- grade energy conversion by using R152a based ORC. They compared the results of experimental and simulation model and found that with a minor bias, a model can predict the steady performance. Ozdil et al. [12] analyzed the thermodynamic performance of ORC system depends on the actual plant data. They found that whenever the temperature of pinch point decreases, exergy performance enhances due to lower exergy destruction rate occurs and finally, they concluded that ORC exergy and energy efficiency of the saturated liquid are 47.22% and 9.96%. Tian et al. [13] projected a transcritical cascade-ORC system to recuperate the multi-grade exhaust waste heat from the weighty diesel engine. They found that maximum heat recovered from the exhaust gas and its recirculation is 153kW and 9.1kW under the conditions of the largest net output of power, thermal efficiency and exergy efficiency found to be 38.2 kW, 11.3%, and 38.7%. Nasir and Kim [14] analyze the thermodynamic performance of seven different working fluids based vapor compression cycle (VCC) powered by ORC for the air cooling purpose. They found that combined R134a based ORC and isobutene based VCC is the best arrangement among other fluids. Long et al. [15] found that thermophysical properties of fluids have little effect on internal exergy efficiency and it goes on increasing with increasing evaporator temperature. They concluded that evaporator temperature greatly influences the selection of organic working liquids in waste heat recovery process. Minea [16] conducted a study on 50kW ORC using waste heat and renewable resources (358.15K to 389.15) to evaluate the technical feasibility and reliability along with the efficiency of heat-to-electricity conversion. This Study concluded that power generation and rate of conversion efficiency in the ORC usually depends on the waste exhaust heat's inlet temperature and cooling liquid. They also found that ORC machine is very reliable and robust for working more than 3000h of continuous operation.

The objective of the current study is to perform an exergy energy analysis of an ORC system used for the recuperation of waste heat from low-temperature sources. In addition, the temperature of waste exhaust heat, the pressure of the evaporator and the mass flow rate of organic liquid on the system performance are examined. Moreover, this study includes the process of performance optimization for ORC system by using response surface methodology (RSM) with the use of Design Expert software.

II. FIGURE DESCRIPTION

Organic Rankine cycle (ORC) has a simple structure with small cost, and it can utilize the low-temperature exhaust waste energy, geothermal energy and concentrated solar thermal power systems for its operation. Diagram of the simple ORC system is shown in Fig. 1, which is operated through the heat transfer from low-temperature waste heat source to an organic working liquid flowing through the evaporator. Then this heated organic fluid goes to the prime mover or turbine, where expansion occurs and pressure reduced. After that organic fluid goes to the condenser unit, where fluid rejects its heat to the cooling medium. Finally, organic fluid after it is being cooled pumped back to the evaporator and this process repeated. Relevant parameters related to the low- temperature ORC are described in Table 1 and the temperature entropy diagram is shown in Fig. 2.

ISSN: 2321-9653; IC Value: 45.98; SJ Impact Factor:6.887
Volume 5 Issue VII, July 2017- Available at www.ijraset.com

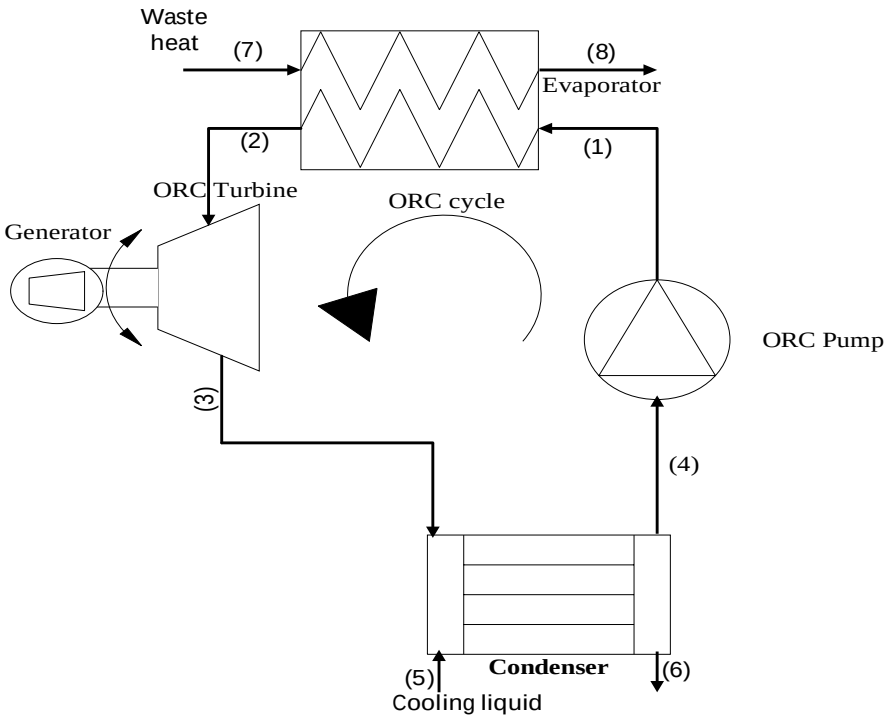

Figure 1. Schematic diagram of the ORC system

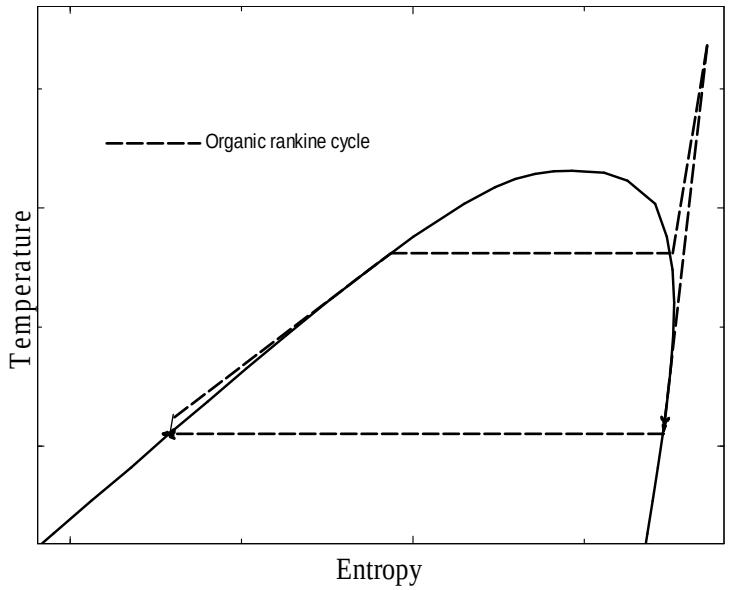

Figure 2. Temperature entropy (T-S) diagram for the ORC system [26]

III. SYSTEM MODELING

This section is divided into two parts: exergy analysis and modeling of ORC is discussed in the first part and response surface methodology (RSM) modeling for optimization of ORC system is discussed in the second part as shown below:

A. Exergy Analysis for the ORC System

Waste heat is used to operate the ORC cycle by exchange of heat through the evaporator. Energy transfer rate from the waste heat can be expressed as:

$$\dot{Q} = \dot{m} C_P (T_7 - T_1) \qquad (1)$$

ISSN: 2321-9653; IC Value: 45.98; SJ Impact Factor:6.887
Volume 5 Issue VII, July 2017- Available at www.ijraset.com

Where $\dot{m}$ is the mass flow rate, and C_P is the specific heat of the liquid having waste heat, T_7 and T_1 are the temperature of the waste exhaust heat and organic liquid entering the evaporator.

For the evaporator (Process 7-8)

The rate of actual energy transferred from the waste heat in the evaporator can be found as:

$$\dot{Q}_{actual} = \dot{m}C_P(T_7 - T_8) \quad (2)$$

Where, T_8 is the temperature of waste heat of liquid that leaves the evaporator.

For turbine (Process 2-3)

The actual rate of work produced by the ORC turbine can be determined as:

$$\dot{W}_{actual,turbine} = \dot{W}_{ideal,turbine}\eta_{turbine} = \eta_{turbine}\dot{m}_{fluid}C_{p,fluid}(T_2 - T_{3s}) = \dot{m}_{fluid}C_{p,fluid}(T_2 - T_3) \quad (3)$$

Where $\dot{m}_{fluid}$ is organic liquid's mass flow rate, $C_{p,fluid}$ is the organic liquid's specific heat, T_2, T_3, and T_{3s} are the inlet, outlet and outlet temperature for ORC turbine in an ideal situation, $\eta_{turbine}$ is ORC turbine's isentropic efficiency and $\dot{W}_{ideal,turbine}$ is ideal power of ORC turbine.

For the condenser (Process 3-4)

The actual rate of energy transferred from organic fluid to cooling fluid can be determined as:

$$\dot{Q}_{actual,condensor} = \dot{m}_{fluid}C_{p,fluid}(T_3 - T_4) \quad (4)$$

For the pump (Process 4-1)

The actual rate of work done in the ORC pump can be determined as:

$$\dot{W}_{actual,pump} = \dot{W}_{ideal,pump}/\eta_{pump} = \dot{m}_{fluid}C_{p,fluid}(T_4 - T_{1s})/\eta_{pump} = \dot{m}_{fluid}C_{p,fluid}(T_4 - T_1) \quad (5)$$

Where $\dot{W}_{ideal,pump}$ is the ideal power of pump, η_{pump} is the isentropic efficiency of the ORC turbine, T_4, T_1, and T_{1s} is the inlet, outlet and outlet temperature of the ORC turbine in ideal situation.

Further net work output from the ORC cycle along with thermal efficiency and exergy efficiency can be estimated as:

$$\dot{W}_{Net} = \dot{W}_{actual,turbine} + \dot{W}_{actual,pump} \quad (6)$$

$$\eta_{thermal} = \frac{\dot{W}_{Net}}{\dot{Q}_{actual}} \quad (7)$$

$$\eta_{exergy,evaporator} = \frac{ex_1 - ex_2}{Ex_{inl}} \quad (8)$$

Where, ex_1 and ex_2 are the exergy flow rate of the working liquid at the inlet as well as an outlet to the evaporator.

$$\eta_{exergy} = \frac{\dot{W}_{Net}}{Ex_{inl}} \quad (9)$$

Or

$$\eta_{exergy} = \left[1 - \frac{ex_{destruction}}{Ex_{inl}}\right] \quad (10)$$

Or

$$\eta_{exergy} = \frac{(ex_{turbine} - ex_{pump})}{Ex_{inl}} \quad (11)$$

Where $ex_{destruction}$ is destructed exergy in ORC system, $ex_{turbine}$ and ex_{pump} are the rate of exergy flow of organic fluid due to turbine and pump, Ex_{inl} is inlet exergy rate due to waste heat fluid. η_{exergy}, $\eta_{thermal}$ and $\eta_{exergy,evaporator}$ is exergy efficiency, thermal efficiency and evaporator exergy efficiency.

$$Ex_{inl} = \dot{E}_7 - \dot{E}_8 \quad (12)$$

Where $\dot{E}_7$ and $\dot{E}_8$ is the rate of exergy at the inlet and outlet of the exhaust waste heat fluid, respectively.

Physical exergy for organic fluid per unit mass flow rate (ex^{ph}) at any stage is defined as under [17]:

$$ex^{ph} = (h - h_0) - T_0(s - s_0) \quad (13)$$

Where h & s are specific enthalpy and specific entropy and environmental (dead) state T_0 = 298K and P_0 =101.325 kPa, respectively.

Table 1. Important ORC parameters used in the calculation

System parameters	Values
Organic turbine efficiency (%)	87
Organic pump efficiency (%)	85
Evaporator effectiveness (%)	95

Minimum pinch point temperature (℃)	5
Quality of organic fluid leaving evaporator	1
Baseline ORC turbine inlet pressure (MPa)	6
Condenser temperature (K)	328

Table 2. Physical and environmental properties as well as security data of the selected working fluids for ORC is adapted from [18, 19, 20, 21, 22].

Working substance	Physical properties data					Security	Environmental properties		
	Type[a]	Weight (kg/kmol)	T_b[b] (℃)	T_c[c] (℃)	P_c[d] (MPa)	Group	Lifetime (years)	ODP[e]	GWP[f]
R134a	W	102	-26.1	101.1	4.06	A1	14	0	1430
R152a	W	66	-24.0	113.3	4.52	A2	1.4	0	124
R123	D	152.93	27.8	183.7	3.668	B1	1.3	0.020	77
R227ea	D	170.3	-16.4	102.8	2.999	A1	38.9	0	3580

[a]W = Wet, D=Dry, [b]T_b = normal boiling temperature, [c]T_c = critical temperature, [d] P_c = critical pressure
[e]ODP = potential of ozone depletion relative to R11, [f] GWP = potential of global warming relative to CO_2

B. Optimization of ORC using Response Surface Methodology (RSM) Modeling

Independent variables like exhaust temperature, Evaporator pressure, and mass flow rate are taken as X_1, X_2 and X_3, respectively. Dependent or response variables are exergy efficiency (Y_1), thermal efficiency (Y_2) and work output (Y_3), respectively. Results of response variables are concluded through the EES software by using 17 different combinations formed in the design matrix. In the current study, there are three levels in Bob-Behnken design matrix, i.e. low, medium and high and these levels are coded as -1, 0 and +1. The level values of assumed independent variables are transferred in coded places as shown in Table 3. For the optimization of process variables, the total numbers of 17 runs are performed randomly as described in Table 4 with the simulation results of the dependent variables: exergy efficiency, thermal efficiency, and work output, respectively. The simulation based data is analyzed by RSM technique through Design Expert software package 8.0.7.1 (Stat Ease Inc., Minneapolis, USA) to fit the data in a second order polynomial equation. Table 5 described the complete design summary of the RSM model.

$$Y_R = \beta_0 + \sum_{m=1}^{n} \beta_m x_m + \sum_{m=1}^{n} \beta_{mm} x_{m^2} + \sum \sum_{m<j}^{n} \beta_{mj x_m x_j} + e_j \qquad (14)$$

Where, Y is the forecasted response corresponds to independent variables X_1, X_2, and X_3, respectively. β_0, β_m and β_{mj} are known by linear, quadratic, and cross-product term coefficient. Furthermore, coded and real values are related to each other as expressed in Eq. (14)

$$Z = \frac{(X - X^0)}{\Delta X} \qquad (15)$$

Where Z denotes the coded values, i.e. -1, 0, and +1, X and X^0 are the uncoded value and mid value of the domain, ΔX shows the augmentation in X for each unit of Z.

Design Expert software is used to perform statistical analysis and the simulation based data is analyzed by regression analysis. F-test is used to check the Significance of regression coefficient. It has been noted that the quadratic model should be suggested during modeling together with linear, squared and interaction terms, whose adequacy concerning the values of R-Squared, Adj R-Squared, and PRESS (prediction error sum of squares) is examined. Pareto analysis of variance (ANOVA) is significantly used to find the response variables, and on behalf of it, tables are also generated.

Table 3. Range and coded levels of independent variables

Independent variables	Range and Levels		
	-1	0	+1
Exhaust temperature X_1 (K)	450	486	522
Evaporator pressure X_2 (MPa)	6	10.50	15
Mass flow rate X_3 (kg/s)	0.10	0.33	0.55

Table 4. Bob-Behnken design matrix along with simulation results

Run	X_1	X_2	X_3	Exergy efficiency (%)				Thermal efficiency (%)				Work output (kJ)			
				R134a	R152a	R123	R227ea	R134a	R152a	R123	R227ea	R134a	R152a	R123	R227ea
1	486	10.5	0.325	57.61	45.35	62.21	61.89	9.079	11.98	5.574	6.439	23.41	30.88	14.37	16.6
2	450	6	0.325	66.09	48.6	45.29	50.96	9.402	11.05	3.609	4.381	24.25	28.5	7.915	11.3
3	486	6	0.1	81.07	72.94	63.8	73.03	4.498	6.761	1.762	2.505	11.6	17.43	4.543	6.459
4	450	15	0.325	35.46	28.08	43.26	40.56	4.116	5.468	2.853	3.146	10.62	14.11	7.36	8.115
5	486	10.5	0.325	57.61	45.35	62.21	61.89	9.079	11.98	5.574	6.439	23.41	30.88	14.37	16.6
6	450	10.5	0.55	39.47	63.47	44.04	42.7	8.037	21.54	4.897	5.696	20.73	55.55	12.63	14.69
7	522	6	0.325	88.06	80.1	76.2	86.94	18.67	28.08	8.714	11.93	48.12	72.36	22.46	30.74
8	486	10.5	0.325	57.61	45.35	62.21	61.89	9.079	11.98	5.574	6.439	23.41	30.88	14.37	16.6
9	486	15	0.1	52.23	41.05	61.31	59.42	2.355	3.125	1.644	1.812	6.073	8.058	4.24	4.672
10	486	15	0.55	52.18	67.12	61.29	59.39	12.95	28.15	9.044	9.966	33.4	72.59	23.32	25.7
11	486	6	0.55	80.99	94.88	63.77	72.99	24.74	48.46	9.691	13.78	63.79	124.9	24.99	35.52
12	450	10.5	0.1	39.51	30.96	44.05	42.72	1.461	1.907	0.8903	1.036	3.769	4.919	2.296	2.671
13	486	10.5	0.325	57.61	45.35	62.21	61.89	9.079	11.98	5.574	6.439	23.41	30.88	14.37	16.6
14	522	10.5	0.1	72.36	59.44	74.07	75.89	4.096	5.551	2.515	2.887	10.55	14.31	6.483	7.44
15	522	15	0.325	65.85	52.94	72.92	73.05	11.55	15.41	8.067	8.856	29.76	39.71	20.79	22.82
16	522	10.5	0.55	72.32	80.97	74.02	75.85	22.51	41.63	13.83	15.88	58.01	107.3	35.66	40.92
17	486	10.5	0.325	57.61	45.35	62.21	61.89	9.079	11.98	5.574	6.439	23.41	30.88	14.37	16.6

X_1= Exhaust temperature (K); X_2= Evaporator pressure (MPa); X_3= Mass flow rate (kg/s)

Table 5. Design summary of the RSM model with simulation data (Design Expert 8.0.7.1)

Study Type	Response Surface	**Runs**	17
Initial Design	Box-Behnken	**Blocks**	No Blocks
Design Model	Quadratic		

Factor	Name	Units	Type	Low Actual	High Actual	Low Coded	High Coded	Mean	Std. Dev.
A	Exhaust temperature	K	Numeric	450.00	522.00	-1.000	1.000	486.000	24.696
B	Evaporator pressure	MPa	Numeric	6.00	15.00	-1.000	1.000	10.500	3.087
C	Mass flow rate	kg/s	Numeric	0.100	0.55	-1.000	1.000	0.325	0.154

Response	Name	Units	Obs	Analysis	Minimum	Maximum	Mean	Std. Dev.	Ratio	Trans	Model
Y1	Exergy efficiency (R134a)	%	17	Polynomial	35.460	88.060	60.802	14.614	2.483	None	Quadratic
Y2	Exergy efficiency (R152a)	%	17	Polynomial	28.080	94.880	55.724	17.912	3.379	None	Quadratic
Y3	Exergy efficiency (R123)	%	17	Polynomial	43.260	76.200	60.886	10.496	1.761	None	Quadratic
Y4	Exergy efficiency (R227ea)	%	17	Polynomial	40.560	86.940	62.526	12.616	2.143	None	Quadratic
Y5	Thermal efficiency (R134a)	%	17	Polynomial	1.461	24.740	9.987	6.415	16.934	None	Quadratic
Y6	Thermal efficiency (R152a)	%	17	Polynomial	1.907	48.460	16.296	12.854	25.412	None	Quadratic
Y7	Thermal efficiency (R123)	%	17	Polynomial	0.890	13.830	5.611	3.310	15.534	None	Quadratic
Y8	Thermal efficiency (R227ea)	%	17	Polynomial	1.036	15.880	6.710	4.091	15.328	None	Quadratic
Y9	Work output (R134a)	kJ	17	Polynomial	3.769	63.790	25.748	16.535	16.925	None	Quadratic
Y10	Work output (R152a)	kJ	17	Polynomial	4.919	124.900	42.008	33.130	25.391	None	Quadratic
Y11	Work output (R123)	kJ	17	Polynomial	2.296	35.660	14.385	8.588	15.531	None	Quadratic
Y12	Work output (R227ea)	kJ	17	Polynomial	2.671	40.920	17.297	10.542	15.320	None	Quadratic

IV. RESULTS AND DISCUSSION

A. Exergy Performance of ORC System

The cycle is replicated by computational numerical technique, i.e. EES software [23] by using cycle data and the relevant parameters related to organic Rankine cycle (ORC) as described in Table 1. Figure 3 shows the effect of exhaust temperature on the thermal and exergy efficiency as well as on the net work output for different working fluids used in the ORC. The selected temperature range should lie under the effective range of low-grade waste heat temperature (i.e. 450K to 522K). It has been demonstrated in figure 3 that with the increase in exhaust waste heat temperature, the exergy efficiency, thermal efficiency as well as net work output of the ORC also increases. It has been concluded that R227ea has a highest exergy

efficiency of around 76.42% at 522K followed by R123, R134a and R152a having an exergy efficiency of 74.21%, 73.66% and 60.87% at 522K. While on the other side R152a demonstrates high thermal efficiency and net work output, i.e. around 22.99% and 59.25kJ at 522K, which is followed by R134a, R227ea, and R123 as illustrated in Fig. 3.

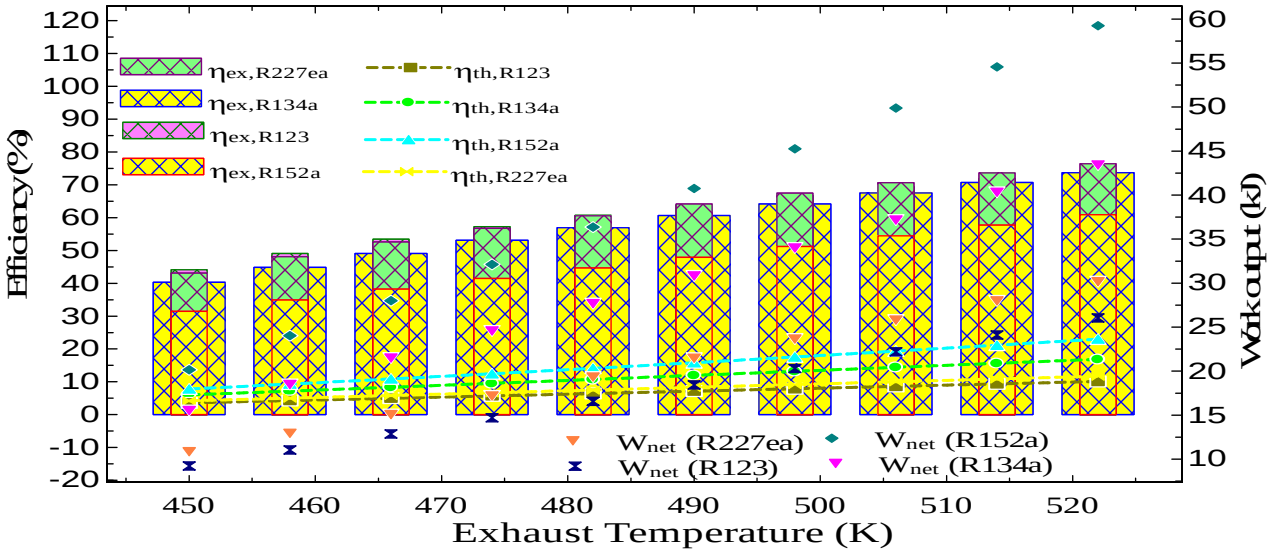

Figure 3. Exergy efficiency, thermal efficiency and net work output versus exhaust temperature

Furthermore, figure 4. illustrates the effect of varying evaporator pressure on the system exergy and thermal efficiency as well as net work output. It has been seen that with increasing evaporator pressure correspondingly exergy and thermal efficiency along with work output of ORC goes on decreases. It has been found that R134a results in highest exergy efficiency, which varies from 66.08% at 6MPa to at 35.46% 15MPa followed by R227ea, R152a, and R123. In addition, Results revealed that R152a shows extreme value of thermal efficiency and net work output, which is around 13.39% and 34.55kJ at 6MPa followed by R134a, R227ea, and R123 as shown in Fig. 4.

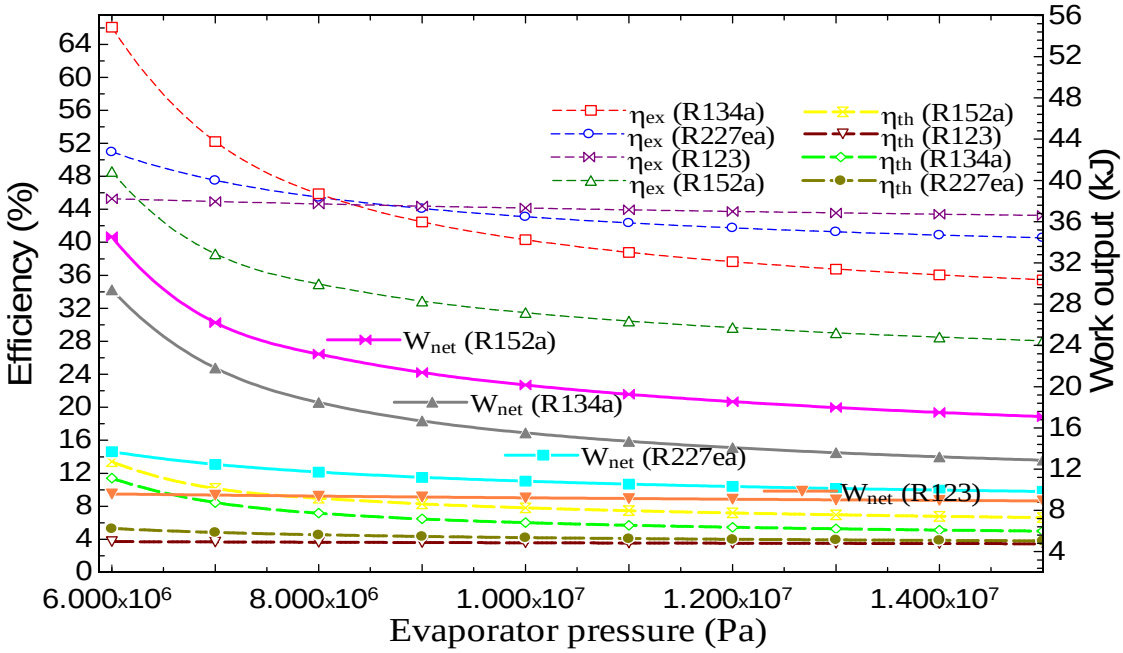

Figure 4. Exergy efficiency, thermal efficiency and net work output versus evaporator pressure

Figure 5 illustrates the effect of exhaust waste heat temperature and pressure of the evaporator on the exergy efficiency of the evaporator. It has been concluded that with the increasing temperature of exhaust waste heat, evaporator exergy efficiency also

increases. On the contrary, the increasing pressure of evaporator has an inverse function of the evaporator exergy efficiency i.e. it goes on decreasing. It has been seen that R227ea possess highest evaporator exergy efficiency value, which varies from 50.6% at 450K to 67.58% at 522K followed by R123, R134a, and R152a. On the other hand, R123 demonstrates the best results of evaporator exergy efficiency, i.e. around 53.85% at 15MPa and 54.37% at 6MPa proceeded by R227ea, R134a, and R152a. It has been also concluded that R123 and R227ea have the marginal difference between the results of evaporator exergy efficiency in the selected range of temperatures (i.e. 450K to 522K) and critical pressure limits (6MPa and 15MPa). Also, Figure 6 demonstrates the effect of mass flow rate on the exergy and thermal efficiency as well as net work output of the ORC. However the effect of mass flow rate on the exergy efficiency not so impressive but it has an accountable effect on thermal efficiency and net work output. It has been found that R123 has highest exergy efficiency, i.e. varies from 44.16% at 0.1kg/s and 44.15% at 0.55kg/s followed by R227ea, R134a, and R152a. Therefore, it has been concluded that there is a minute dissimilarity between the exergy efficiency values with the variation in mass flow rate of the working fluid. On the other hand, with the increasing mass flow rate, thermal efficiency and net work output also increase. It is clearly understood from the figure 6 that R152a possess highest thermal efficiency value and net work output i.e. around 10.75% and 27.72kJ at 0.55kg/s followed by R134a, R227ea, and R123. Finally, the results revealed from exergy energy analysis that temperature of waste heat gasses, evaporator pressure as well as mass flow rate are important parameters to achieve better system performance. Therefore, during the designing of the ORC system, these parameters must be considered to recuperate the waste heat from the waste heat temperature source to generate power. Lastly, Table 5(a) provides the exergetic performance information about some important organic fluids such as R1234yf and R1234ze. Due to its less global warming potential of these organic fluids, they are potentially utilized in these days.

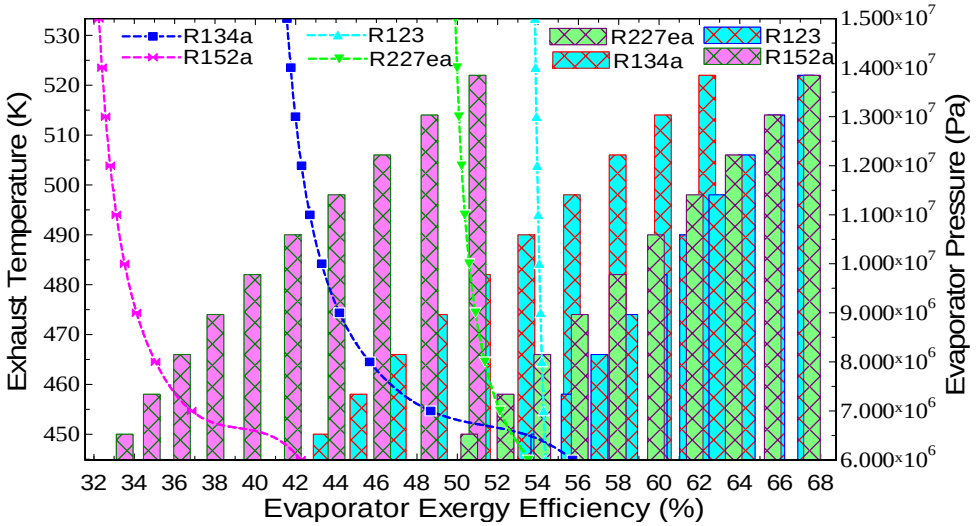

Figure 5. Variations in evaporator exergy efficiency with respect to exhaust temperature and evaporator pressure

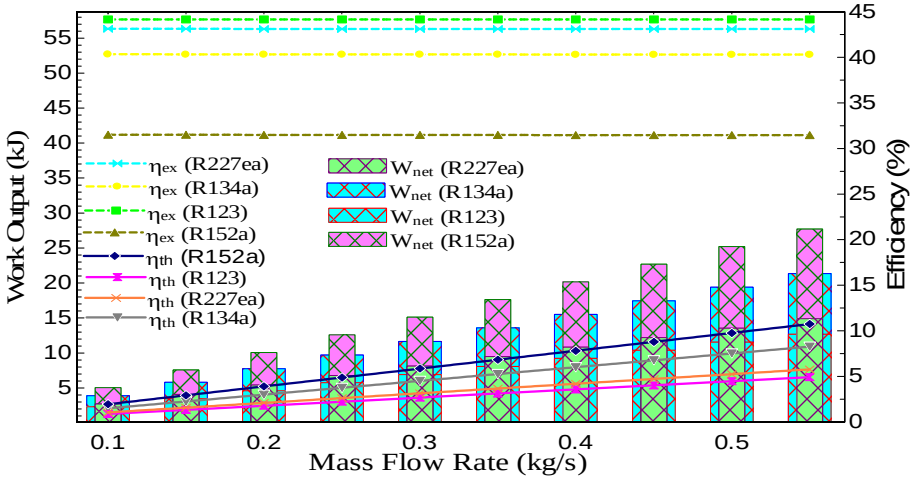

Figure 6. Exergy efficiency, thermal efficiency and net work output versus mass flow rate

ISSN: 2321-9653; IC Value: 45.98; SJ Impact Factor:6.887
Volume 5 Issue VII, July 2017- Available at www.ijraset.com

Table 5(a) Exergy efficiency values for organic fluids at 0.1kg/s

Fluid	Exergy efficiency
R1234yf	60.96%
R1234ze	60.71%

B. RSM Modeling and Optimization Results

The results of simulation based experiments performed according to the arrangements formed in BBD (Box-Behnken Design) are shown in Table 4 including the study of process parameters on the exergy efficiency, thermal efficiency and work done, respectively. These response variables are utilized to develop the statistical model by using the method of multiple regression analysis to fit the response function in accordance with Eq. (14). The relationship between independent variables and response variables are described in Table 6. F-test analysis of variance is used to evaluate the significance of the statistical model. It has been observed from the Table 7 that the quadratic model of the response variable (i.e. Exergy efficiency of R134a) is significant at 99.9% confidence level due to the value of "Prob>F" less than 0.0001 and the F value of the model is 111.55. It has been also observed that all other models correspond to response variables for selected working fluids are significant due to the same reason of "Prob>F" less than 0.0001. Model's adequacy can be checked by R-Squared, Adj R-Squared, Pred R-Squared and prediction error sum of squares (PRESS) [24] and these values are described in Table 7.

Table 6. The fitted model equations for actual and coded factors

(a) Final equations in terms of coded factors	(b) Final equations in terms of actual factors
Exergy efficiency (R134a) =+57.61+14.76*A-13.81*B-0.026*C+2.10*A*B+0.000*A*C+7.500E-003*B*C-2.22 *A^2+8.48*B^2+0.53*C^2 Exergy efficiency (R152a) =+45.35+12.79*A-13.42*B+12.76*C-1.66*A*B-2.75*A*C+1.03*B*C-1.60*A^2+8.68*B^2+14.96*C^2 Exergy efficiency (R123) =+62.21+15.07*A-1.29*B-0.014* C-0.31*A*B-1.000E-002*A*C+2.500E-003*B*C-3.15 *A^2+0.35*B^2-0.020*C^2 Exergy efficiency (R227ea) =+61.89+16.85*A-6.44*B-0.016* C-0.87*A*B-5.000E-003*A*C+2.500E-003*B*C-2.97*A^2+3.95*B^2+0.37*C^2 Thermal efficiency (R134a) =+9.08+4.23*A-3.29*B+6.98 *C-0.46*A*B+2.96*A*C-2.41*B*C-0.13*A^2+1.98*B^2+0.074*C^2 Thermal efficiency (R152a) =+11.98+6.34*A-5.27*B+15.30*C-1.77*A*B+4.11*A*C-4.17*B*C-0.47*A^2+3.49*B^2+6.15*C^2 Thermal efficiency (R123) =+5.57+2.61*A-0.27*B+3.83*C+0.027*A*B+1.83*A*C-0.13*B*C+0.12*A^2+0.12*B^2-0.16*C^2 Thermal efficiency (R227ea) =+6.44+3.16*A-1.10*B+4.64*C-0.46*A*B+2.08*A*C-0.78*B*C-8.750E-004*A^2+0.64*B^2-0.063*C^2 Work output (R134a) =+23.41+10.88*A-8.49*B+17.99*C-1.18*A*B+7.62*A*C-6.22*B*C-0.34* A^2+5.11*B^2+0.19*C^2	Exergy efficiency (R134a), Y_1 =-401.03247+1.94131*X_1-18.17935*X_2 -6.98333*X_3+0.012994* X_1* X_2+ 0.000000 *X_1*X_3+7.40741E-003*X_2*X_3-1.71586E-003*X_1^2+ 0.41870*X_2^2+10.44444*X_3^2 Exergy efficiency (R152a), Y_2 =-430.59203+1.77589*X_1-7.33 818*X_2+18.55988*X_3-0.010247*X_1*X_2 -0.33889* X_1*X_3 +1.01975*X_2*X_3-1.23746E-003*X_1^2+0.42883*X_2^2+ 295.58025*X_3^2 Exergy efficiency (R123), Y_3= 719.56282+2.79805*X_1+0.28559*X_2+0.76975*X_3-1.92901E-003*X_1*X_2-1.23457 E-003 *X_1*X_3+2.46914E-003*X_2*X_3-2.42670E-003*X_1^2+0.017 407*X_2^2-0.39506*X_3^2 Exergy efficiency (R227ea), Y_4=-696.18718+2.74852*X_1-2.91275*X_2-4.48457* X_3-5.38580E-003*X_1*X_2-6.17284 E-004*X_1*X_3+2.46914E-003*X_2*X_3-2.28781E-003*X_1^2 +0.19519*X_2^2+7.20988*X_3^2 Thermal efficiency (R134a), Y_5 =-27.45362+0.12371*X_1-0.63805*X_2-122.49599*X_3-2.83025E-003*X_1*X_2+0.36537*X_1*X_3-2.38198* X_2*X_3 -9.80903E-005*X_1^2+0.097 907*X_2^2+1.46420*X_3^2 Thermal efficiency (R152a), Y_6 =-127.33534+0.48032* X_1+1.85794*X_2-214.39765*X_3 -0.0109 38*X_1*X_2+0.50759*X_1*X_3-4.11704*X_2*X_3-3.645 83E-004*X_1^2+0.17257 *X_2^2+121.47160*X_3^2 Thermal efficiency (R123), Y_7 =+23.17931-0.090552*X_1-0.2 2341*X_2-89.19348*X_3 +1.68210E-004*X_1*X_2+0.22556* X_1*X_3-0.13062*X_2*X_3+9.04996E-005*X_1^2+5.89938

Work output (R152a) =+30.88+16.33*A-13.59*B+39.45 *C-4.56*A*B+10.59*A*C-10.73*B*C-1.22*A^2+9.01* B^2+15.86*C^2 Work output (R123) =+14.37+6.90*A-0.52*B+9.88*C-0. 28*A*B+4.71*A*C-0.34*B*C+0.13*A^2+0.13*B^2-0.23* C^2 Work output (R227ea) =+16.60+8.14*A-2.84*B+11.95*C -1.18*A*B+5.37*A*C-2.01*B*C-6.875E-003*A^2+1.65* B^2-0.16*C^2	E-003*X_2^2-3.12519*X_3^2 Thermal efficiency (R227ea), Y_8 =-13.66370+0.034694 *X_1+0.72098* X_2 -95.48870*X_3-2.83796E-003*X_1*X_2+ 0.25719*X_1*X_3-0.77062*X_2*X_3-6.75154E- 007*X_1^2+0.031611 *X_2^2-1.25185*X_3^2 Work output (R134a), Y_9 =-72.34930+0.32560*X_1-1.647 29* X_2-315.51858*X_3-7.29938E-003*X_1*X_2+0.94133*X_1 *X_3-6.13901*X_2*X_3-2.59838E-004* X_1^2+0.25256*X_2^2+ 3.7 8272* X_3^2 Work output (R152a), Y_{10} =-328.00453+1.23749*X_1+4.7 7960 *X_2-552.31580*X_3-0.028179* X_1*X_2+1.30738*X_1* X_3-10.60198*X_2*X_3-9.39333E-004*X_1^2+0.44481*X_2^2+3 13. 22716*X_3^2 Work output (R123), Y_{11} =+13.62085-0.075024*X_1+0.69 076*X_2-232.23302*X_3-1.72068E-003*X_1*X_2+0.58157* X_1*X_3 -0.33753*X_2*X_3+9.84761E-005*X_1^2+6.59877E- 003*X_2^2 -4.55062*X_3^2 Work output (R227ea), Y_{12} =-36.00547+0.092803*X_1+ 1.85323*X_2-245.89302*X_3-7.30710E-003*X_1*X_2+0.662 38* X_1* X_3-1.98346* X_2*X_3-5.30478E-006*X_1^2+0.08151 2*X_2^2-3.21728*X_3^2
Note A= Exhaust temperature, B= Evaporator pressure, and C= Mass flow rate	Note X_1 = Exhaust temperature, X_2 = Evaporator pressure, and X_3 = Mass flow rate

Table 7. Pareto analysis of variance (ANOVA) of the fitted model based on simulation results

Source	Sum of Squares	df	Mean Square	F Value	Prob > F
For Exergy efficiency (R134a), Y_1					
Model	3605.29	9	400.59	111.55	< 0.0001
Residual	25.14	7	3.59		
Lack of Fit	25.14	3	8.38		
Pure Error	0.000	4	0.000		
Cor Total	3630.43	16			
R-Squared=0.9931, Adj R-Squared=0.9842, Pred R-Squared=0.8892, Adeq Precision=39.313, C.V. %=3.12, PRESS= 402.19, Std. Dev.=1.89, Mean=60.80					
For Exergy efficiency (R152a), Y_2					
Model	5418.26	9	602.03	117.31	<0.0001
Residual	35.92	7	5.13		
Lack of Fit	35.92	3	11.97		
Pure Error	0.000	4	0.000		
Cor Total	5454.18	16			
R-Squared=0.9934, Adj R-Squared=0.9849, Pred R-Squared=0.8946, Adeq Precision=38.134, C.V. %=4.07, PRESS= 574.77, Std. Dev.=2.27, Mean=55.72					
For Exergy efficiency (R123), Y_3					
Model	1872.67	9	208.07	26446.10	<0.0001
Residual	0.055	7	$7.868*10^{-3}$		
Lack of Fit	0.055	3	0.018		
Pure Error	0.000	4	0.000		

Cor Total	1872.72	16			

R-Squared=1.0000, Adj R-Squared=0.9999, Pred R-Squared=0.9995, Adeq Precision=480.850, C.V. %=0.15, PRESS= 0.88, Std. Dev.=0.089, Mean=60.89

For Exergy efficiency (R227ea), Y_4

Model	2704.24	9	300.47	1279.67	<0.0001
Residual	1.64	7	0.23		
Lack of Fit	1.64	3	0.55		
Pure Error	0.000	4	0.000		
Cor Total	2705.88	16			

R-Squared=0.9994, Adj R-Squared=0.9986, Pred R-Squared=0.9903, Adeq Precision=125.315, C.V. %=0.77, PRESS= 26.30, Std. Dev.=0.48, Mean=62.53

For Thermal efficiency (R134a), Y_5

Model	695.02	9	77.22	117.89	<0.0001
Residual	4.59	7	0.66		
Lack of Fit	4.59	3	1.53		
Pure Error	0.000	4	0.000		
Cor Total	699.60	16			

R-Squared=0.9934, Adj R-Squared=0.9850, Pred R-Squared=0.8951, Adeq Precision=37.112, C.V. %=8.10, PRESS= 73.37, Std. Dev.=0.81, Mean=9.99

For Thermal efficiency (R152a), Y_6

Model	2788.27	9	309.81	105.68	<0.0001
Residual	20.52	7	2.93		
Lack of Fit	20.52	3	6.84		
Pure Error	0.000	4	0.000		
Cor Total	2808.79	16			

R-Squared=0.9927, Adj R-Squared=0.9833, Pred R-Squared=0.8831, Adeq Precision=35.216, C.V. %=10.51, PRESS= 328.34, Std. Dev.=1.71, Mean=16.30

For Thermal efficiency (R123), Y_7

Model	186.14	9	20.68	2495.72	<0.0001
Residual	0.058	7	$78.287*10^{-3}$		
Lack of Fit	0.058	3	0.019		
Pure Error	0.000	4	0.000		
Cor Total	186.20	16			

R-Squared=0.9997, Adj R-Squared=0.9993, Pred R-Squared=0.9950, Adeq Precision=184.503, C.V. %=1.62, PRESS= 0.93, Std. Dev.=0.091, Mean=5.61

For Thermal efficiency (R227ea), Y_8

Model	283.95	9	31.55	376.59	<0.0001
Residual	0.59	7	0.084		
Lack of Fit	0.59	3	0.20		
Pure Error	0.000	4	0.000		
Cor Total	284.53	16			

R-Squared=0.9979, Adj R-Squared=0.9953, Pred R-Squared=0.9670, Adeq Precision=70.245, C.V. %=4.31, PRESS= 9.38, Std. Dev.=0.29, Mean=6.71

For Work output (R134a), Y_9

Model	4617.57	9	513.06	117.55	<0.0001
Residual	30.55	7	4.36		
Lack of Fit	30.55	3	10.18		
Pure Error	0.000	4	0.000		
Cor Total	4648.13	16			

R-Squared=0.9934, Adj R-Squared=0.9850, Pred R-Squared=0.8948, Adeq Precision=37.071, C.V. %=8.11, PRESS= 488.83, Std. Dev.=2.09, Mean=25.75

For Work output (R152a), Y_{10}

Model	18522.54	9	2058.06	105.83	<0.0001
Residual	136.13	7	19.45		
Lack of Fit	136.13	3	45.38		
Pure Error	0.000	4	0.000		
Cor Total	18658.68	16			

R-Squared=0.9927, Adj R-Squared=0.9833, Pred R-Squared=0.8833, Adeq Precision=35.240, C.V. %=10.50, PRESS= 2178.15, Std. Dev.=4.41, Mean=42.01

For Work output (R123), Y_{11}

Model	1253.74	9	139.30	12221.14	<0.0001
Residual	0.080	7	0.011		
Lack of Fit	0.080	3	0.027		
Pure Error	0.000	4	0.000		
Cor Total	1253.82	16			

R-Squared=0.9999, Adj R-Squared=0.9999, Pred R-Squared=0.9990, Adeq Precision=409.815, C.V. %=0.74, PRESS= 1.28, Std. Dev.=0.11, Mean=14.38

For Work output (R227ea), Y_{12}

Model	1885.48	9	209.50	375.81	<0.0001
Residual	3.90	7	0.56		
Lack of Fit	3.90	3	1.30		
Pure Error	0.000	4	0.000		
Cor Total	1889.38	16			

R-Squared=0.9979, Adj R-Squared=0.9953, Pred R-Squared=0.9670, Adeq Precision=70.172, C.V. %=4.32, PRESS= 62.43, Std. Dev.=0.75, Mean=17.30

For the evaluation of model's adequacy and fitness, the coefficient of determination R-Squared.(R^2) and Adj R-Squared (Adj R^2) can be used. Additionally, for the sample size and model number of terms, the R^2 value is corrected by Adj R^2.value. In Table 7, observed values of R^2 and Adj R^2 are very high for each model, which implies that up to how much percentage of simulated data is compatible and to advocate for a high importance of the model. Furthermore, the coefficient of variation (CV%) represents the virtual diffusion of experimental points from the estimates of second order polynomial (SOP) [25]. Pred R-Squared (Pred R^2) indicates that overall mean is a superior forecaster of a response than the existing model and Adeq Precision measures the signal to noise ratio, whose value should be greater than 4 that is desirable and in this case, the ratio is found to be larger than 35 refers to an adequate signal. The distribution of residual values publicized by normal probability plots which indicates the difference between the simulation data and forecasted data of all the response variables of exergy efficiency, thermal efficiency and work output of ORC are shown in Fig. 7 (A-L).

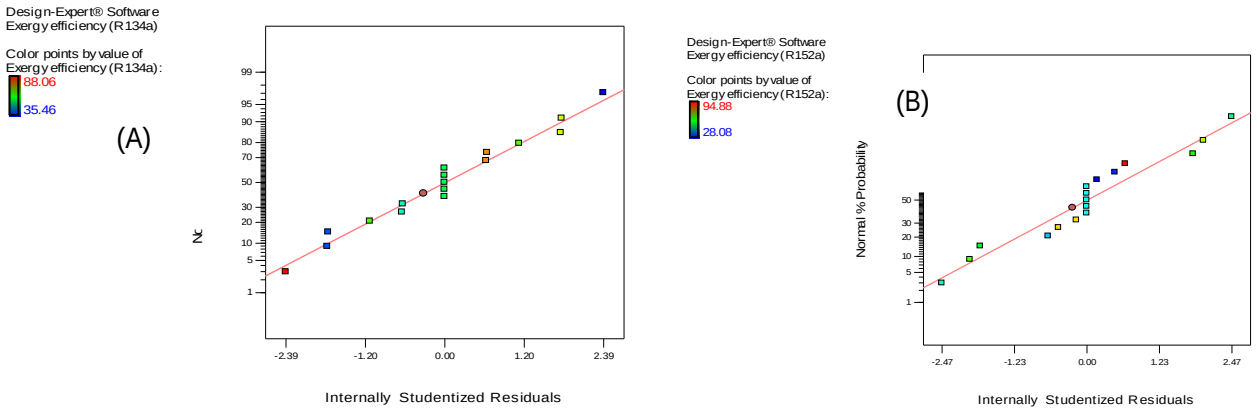

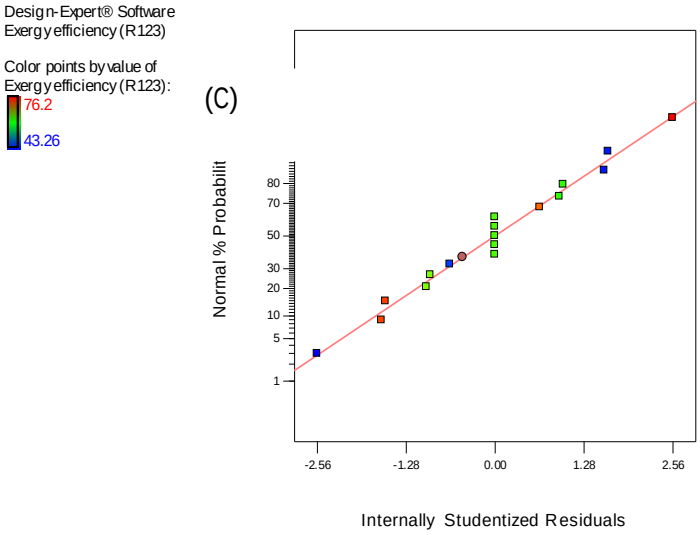

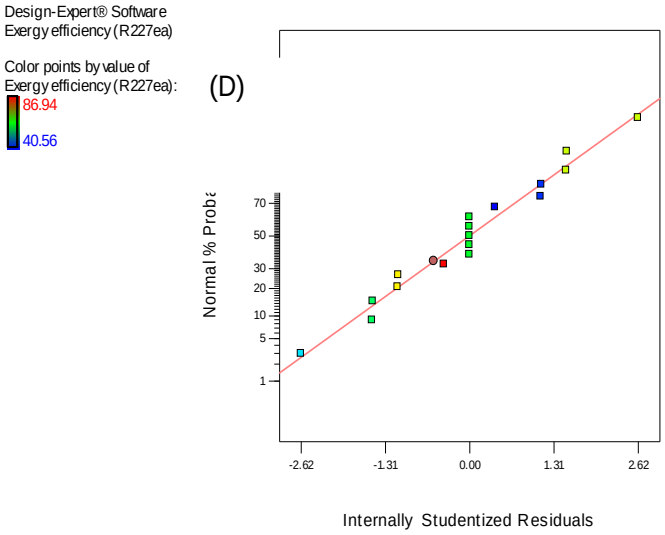

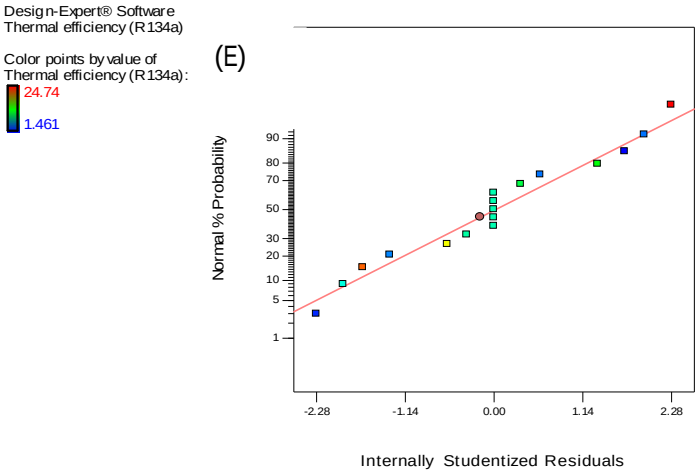

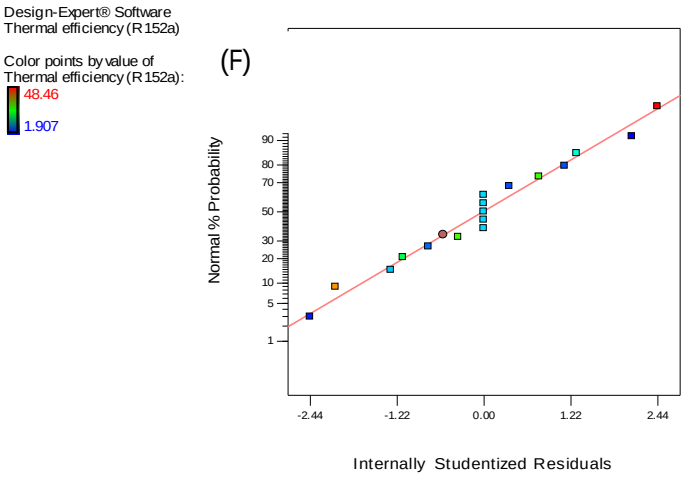

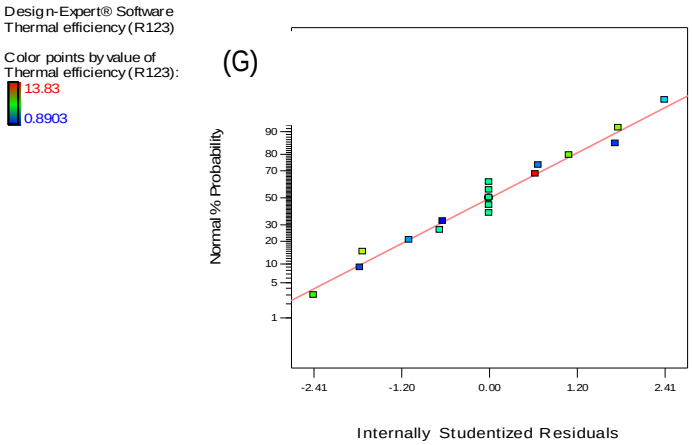

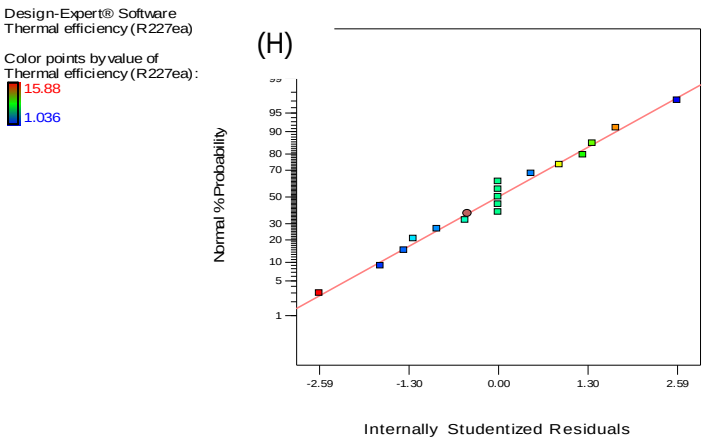

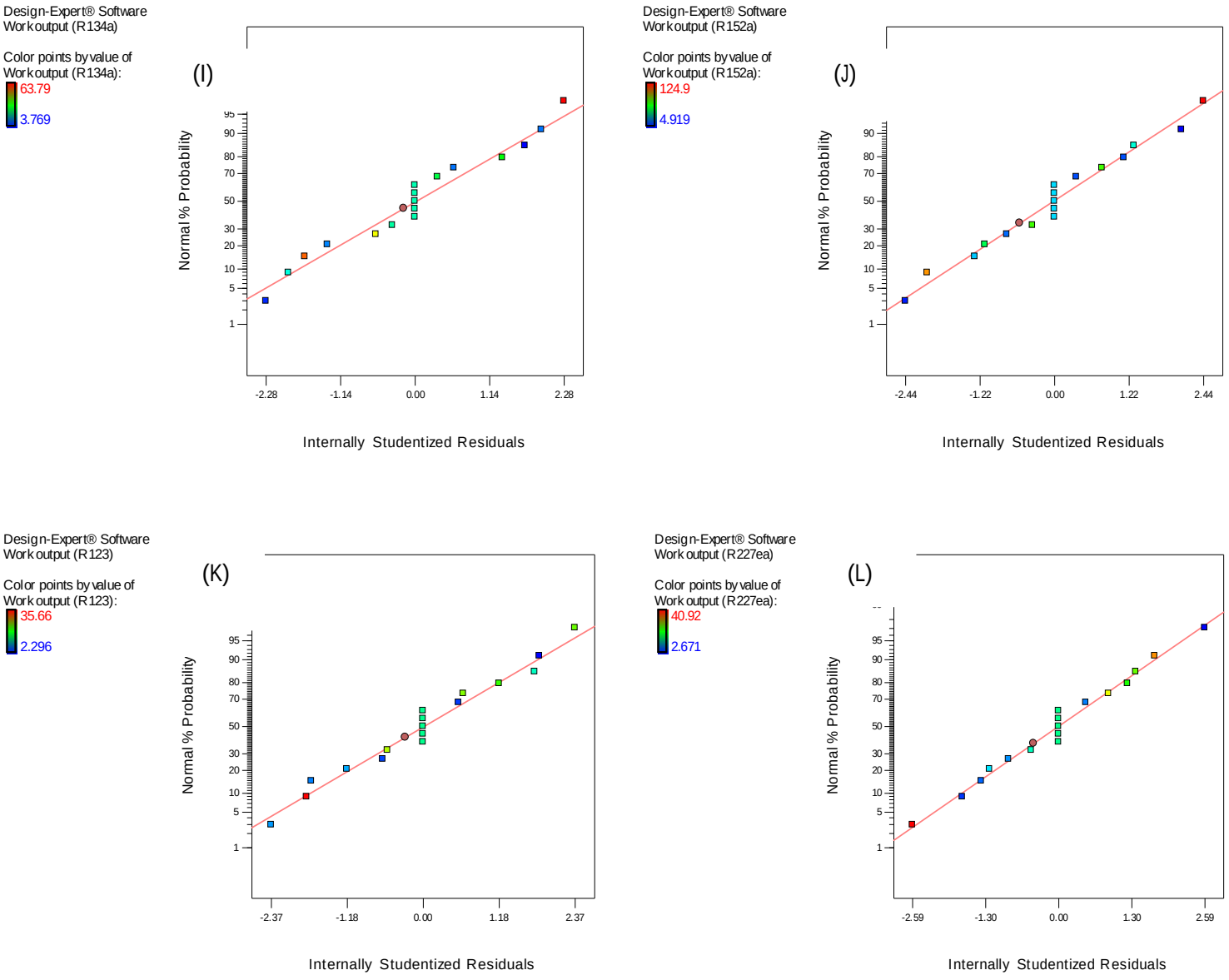

Figure 7. Plots of normal % probability for exergy efficiency (A-D), thermal efficiency (E-H) and work output (I-L) for different models

1) Response Surface and Contour Plots for the Models : Each response surface model is a function of two independent variables at a time, while other factor or variables are considered to be constant or taken up at predetermined positions are more accommodating in accepting the both core and interactive effects of two independent aspects. For the understanding of the relations of variables and the most advantageous level of each variable can be readily determined by response surface curves that are plotted to analyze the maximum value of each response. The response surface models for exergy efficiency, thermal efficiency and work output of ORC for selected working fluids are shown in figure 8, and this indicates the effect of process or independent variables such as exhaust temperature, evaporator pressure and mass flow rate on the responses. It has been analyzed that exergy efficiency increases very rapidly with the increase in exhaust temperature and a decrease in evaporator pressure, while the mass flow rate of working fluid has a less significant effect on the exergy efficiency as shown in Fig 8 (A-L). On the other hand, thermal efficiency increases with increases in both exhaust temperature and mass flow rate and, with the decrease in evaporator pressure as illustrated in Fig 8 (M-X). Moreover, work output of the cycle follows the same trend of thermal efficiency, which means that work output enhances significantly with increases in both exhaust temperature and mass

flow rate and, with the decrease in evaporator pressure as shown in Fig. 8 (a-l). Therefore, it has been concluded that responses value is optimized at the maximum value of both exhaust temperature (i.e. 522K) and mass flow rate (i.e. 0.55kg/s) and less value of evaporator pressure appr y 6MPa, respectively.

(B)

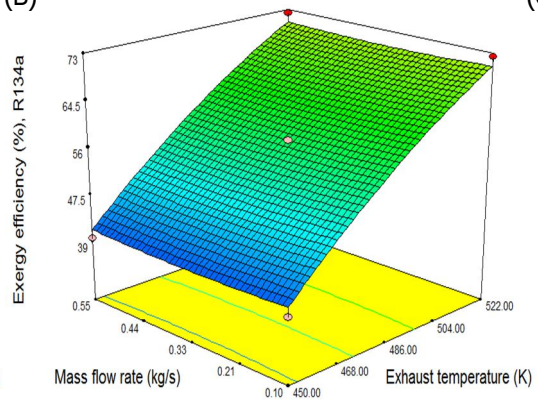

(C)

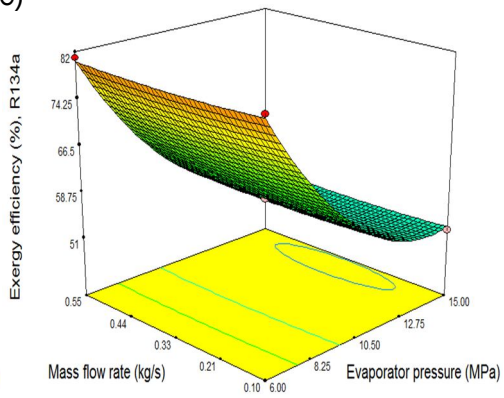

(E)

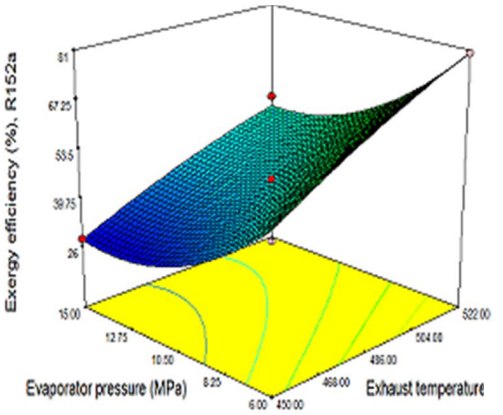

(F)

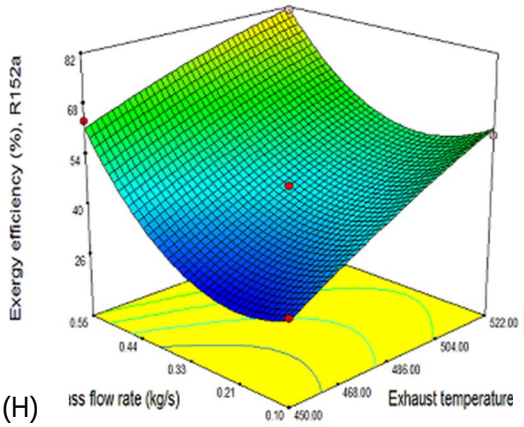

(H)

(I)

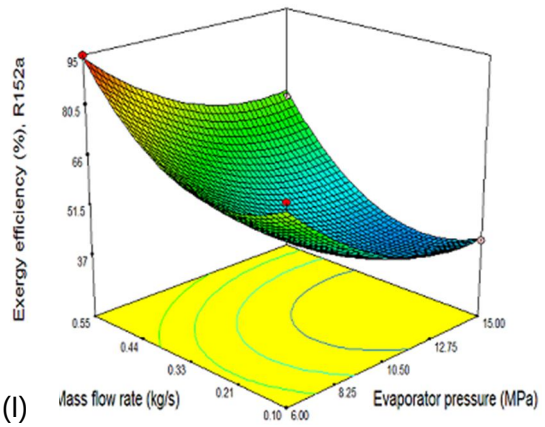

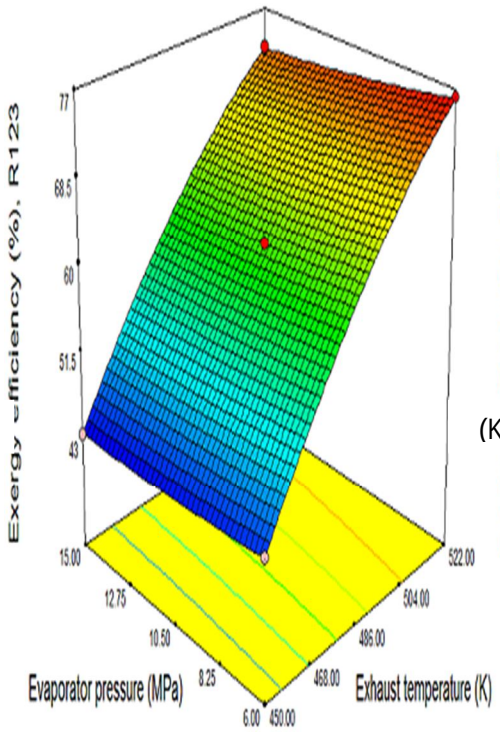

(K)

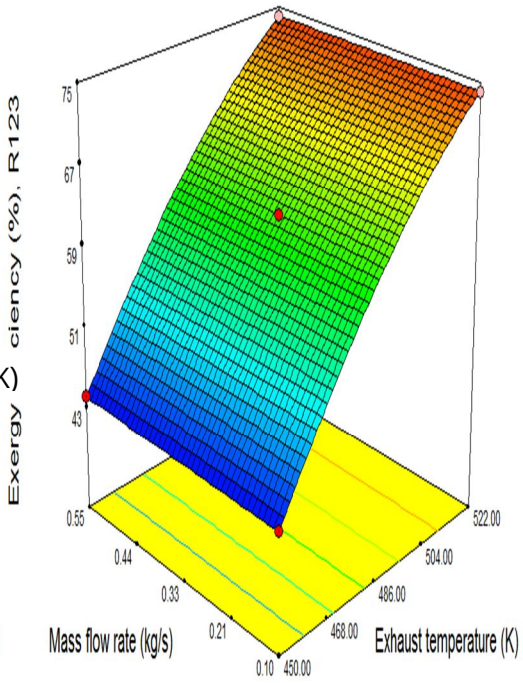

(L)

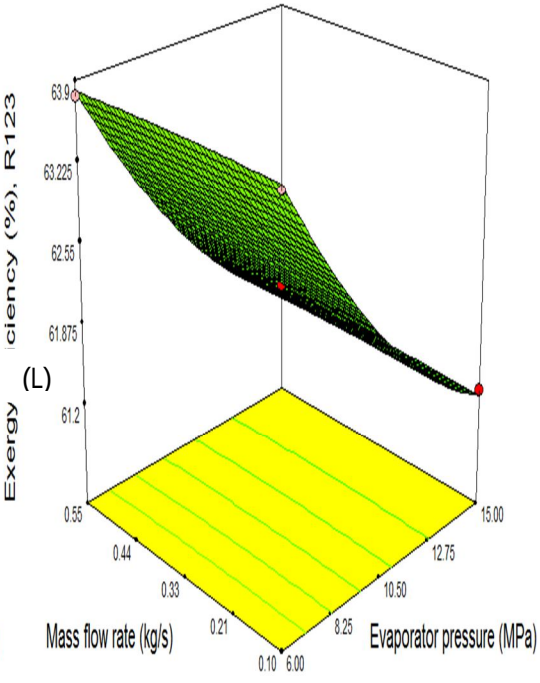

ISSN: 2321-9653; IC Value: 45.98; SJ Impact Factor:6.887
Volume 5 Issue VII, July 2017- Available at www.ijraset.com

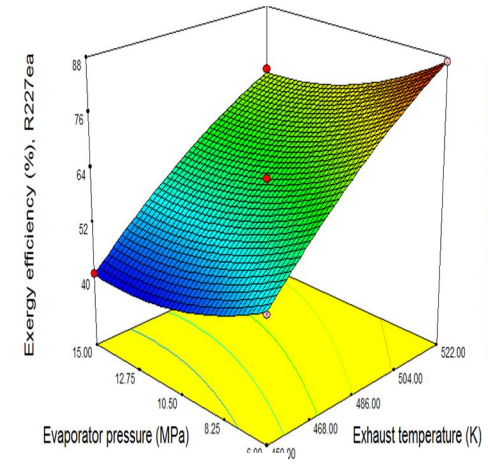

(**M**)

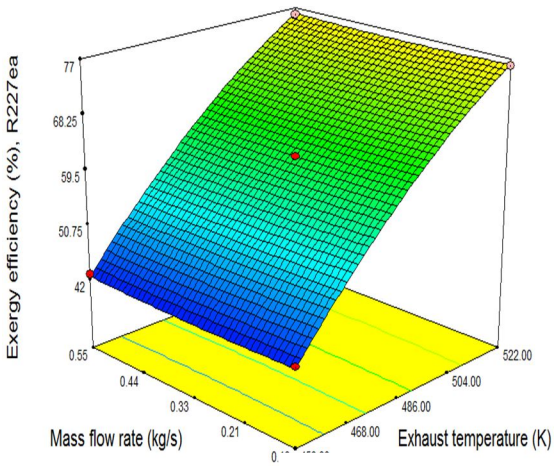

(N)

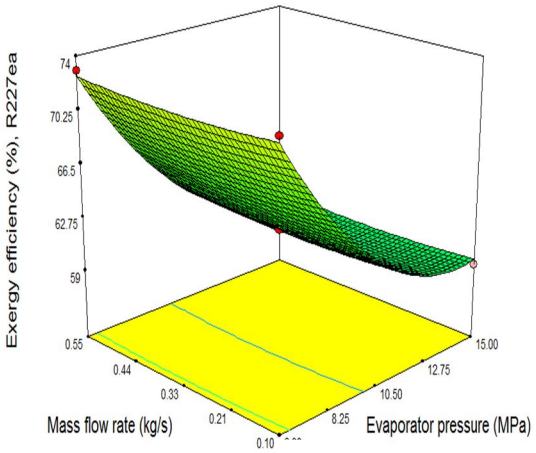

(O)

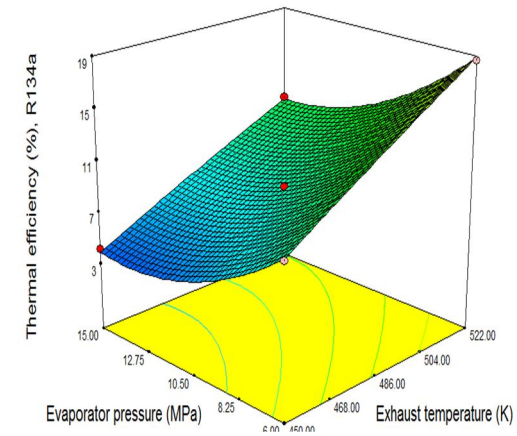

(P)

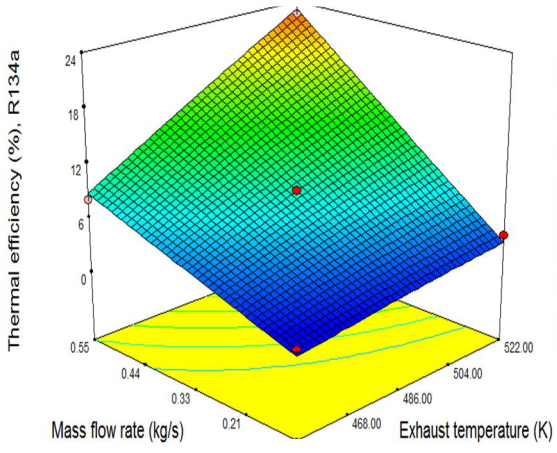

(Q)

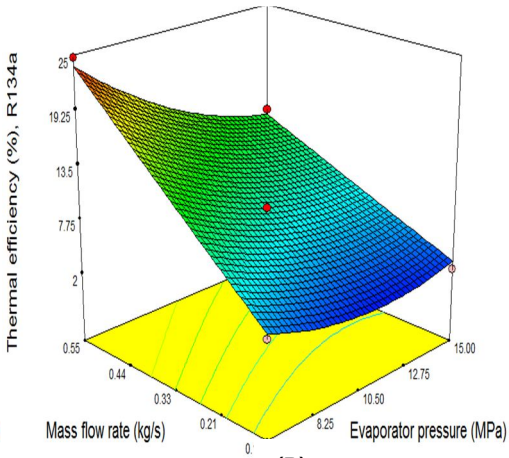

(R)

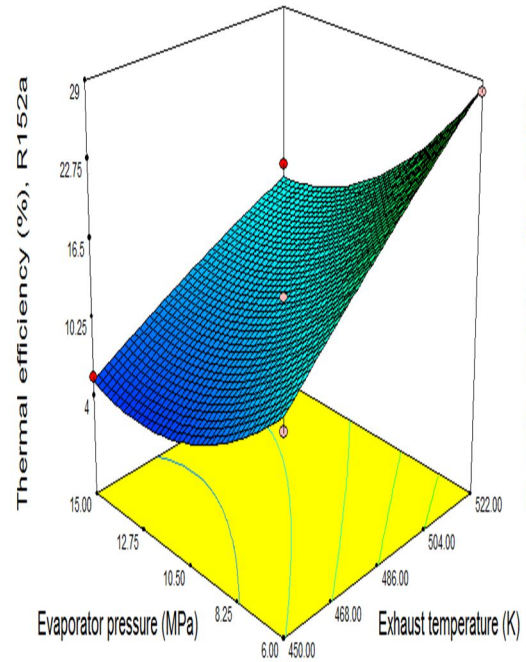

(S)

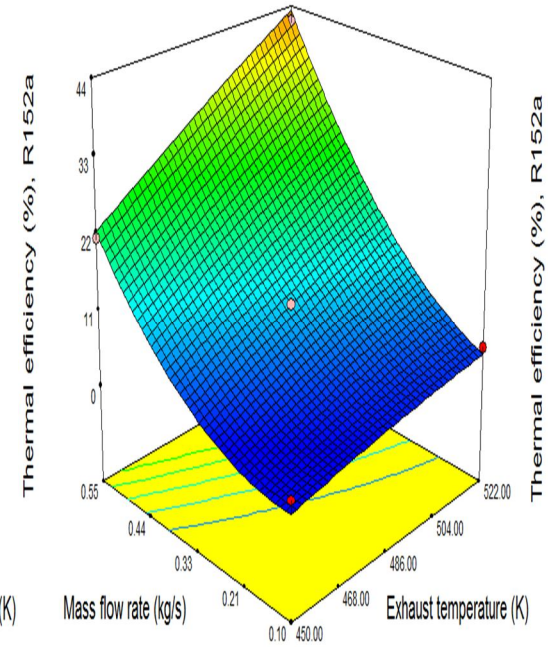

(T)

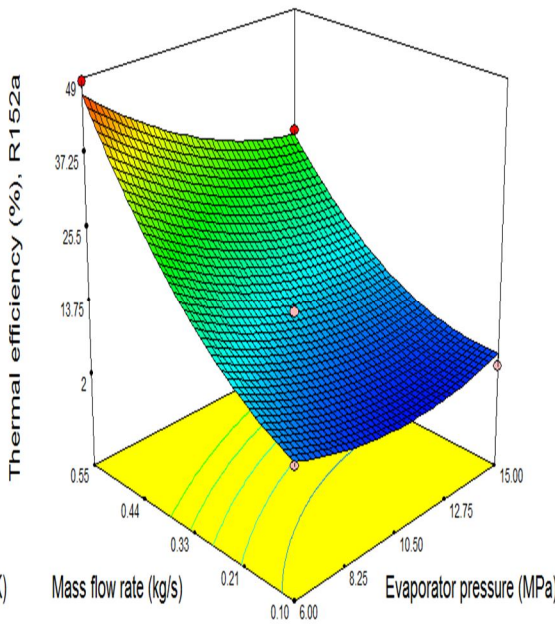

(U)

ISSN: 2321-9653; IC Value: 45.98; SJ Impact Factor:6.887
Volume 5 Issue VII, July 2017- Available at www.ijraset.com

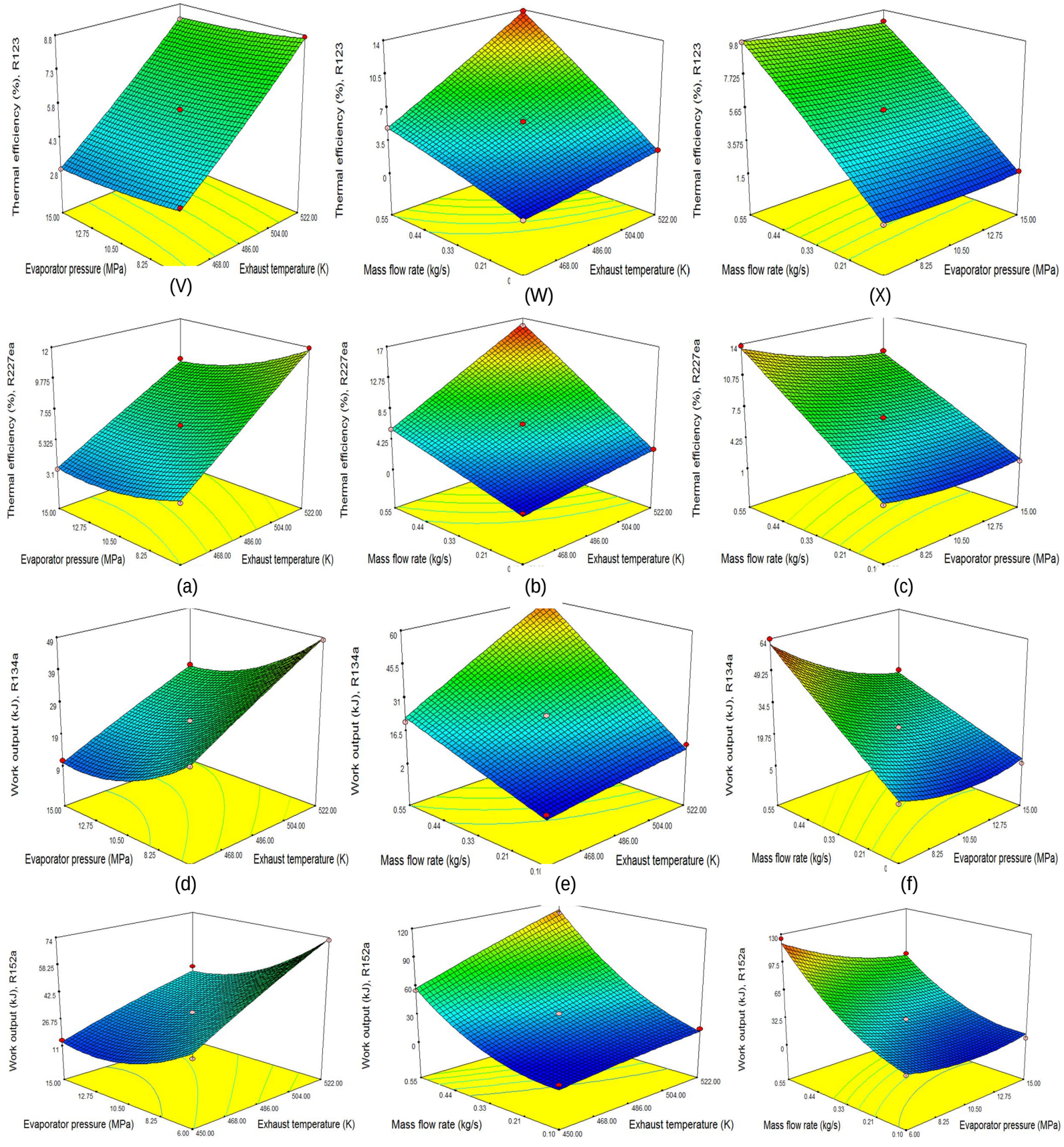

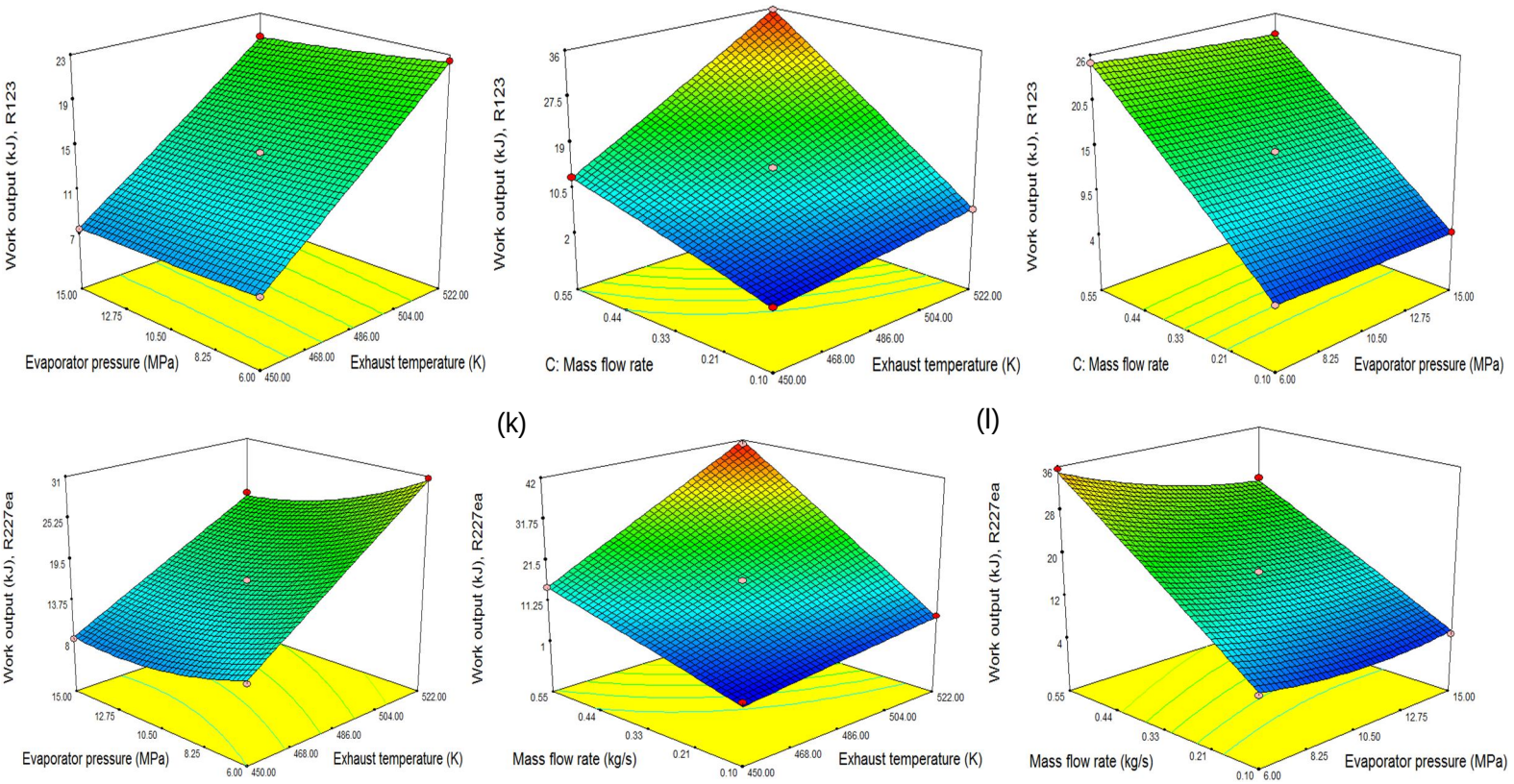

Figure 8. Responses surface plots for Exergy efficiency 8 (A-L), Thermal efficiency 8 (M-X) and Work output 8 (a-l).

2)Optimization using the Desirability Function : In the process of optimization of multiple responses, a second-order polynomial models formed in this study so as to acquire the particular optimum conditions. In order to optimize the exergy efficiency, thermal efficiency and work output of the ORC, the following constraints taken in the range (1) Exhaust temperature (450K-522K), (2) Evaporator pressure (6MPa-15MPa), (3) Mass flow rate (0.1kg/s to 0.55kg/s). The value of response variables must be as high as possible and therefore, it is necessary to institute the most favorable criteria in accordance to the Derringer and Suich (1980) Desirability function (DF) method. This method is used to optimize the process variables for the optimum conditions, i.e. the exhaust temperature of 522K, evaporator pressure of 6.87MPa and mass flow rate is 0.55kg/s, respectively. All the results related to the exergy efficiency, thermal efficiency and work output are found to be under optimum conditions with overall desirability value of 0.990. Finally, it has been found that at the optimum conditions, the optimized value of exergy efficiency for R134a, R152a, R123 and R227ea are observed as 85.58%, 98.47%, 75.60%, and 84.57%; the optimized value of thermal efficiency for R134a, R152a, R123, and R227ea are observed as 29.44%, 54.72%, 14.18%, and 18.55%; the optimized value of work output for R134a, R152a, R123, and R227ea are concluded as 75.89kJ, 141.027kJ, 36.766kJ, and 47.82kJ, respectively.

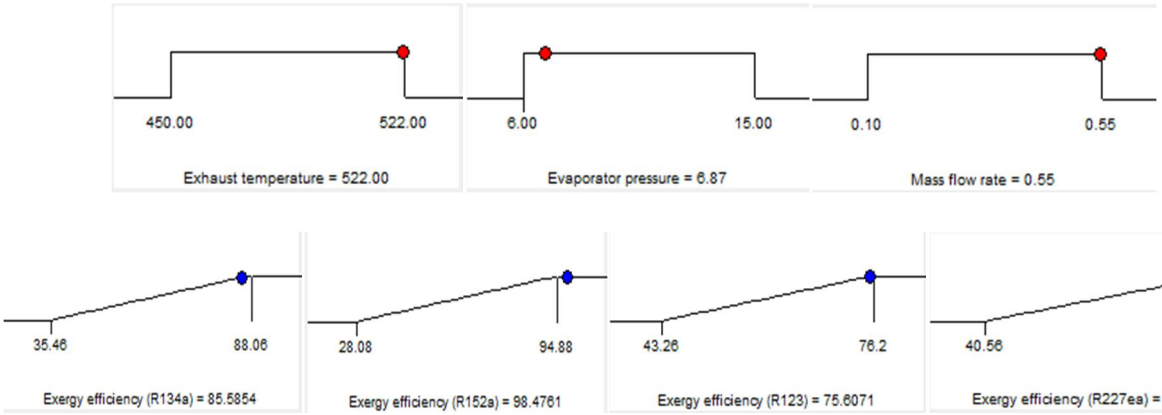

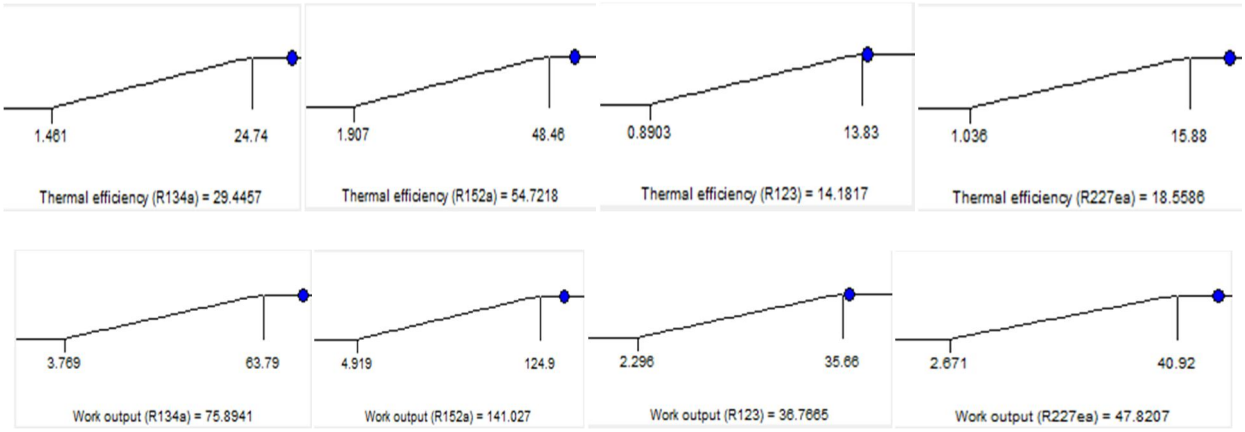

Figure 9. Desirability ramps for optimization of responses (Design Expert software 8.0.7.1)

V. CONCLUSION

This study presented an exergetic energetic analysis of an ORC system integrated by low-grade exhaust waste heat sources to generate power. In addition, the effect of the temperature of exhaust waste heat, the pressure of the evaporator as well as the mass flow rate of the working organic fluid on the exergy efficiency, the thermal efficiency of the system and net work output as well as evaporator exergy efficiency was studied. It was found that recovering waste heat from ORC system with the selected organic fluids was able to generate net work output between 9.22kJ to 20.16kJ at 450K. For the highest temperature of the exhaust waste heat (i.e. 522K) the ORC was able to produce between 26.04kJ to 59.25kJ. Moreover, evaporator pressure and mass flow rate parameters both have a greater impact on the system performance. Therefore, it has been concluded that an ORC system with the selected organic fluids was able to generate net work output between 9.594kJ to 34.55kJ at an evaporator pressure of 6MPa and 12.68kJ to 27.72kJ at a mass flow rate of 0.55kg/s. So designers have to select the optimum value of all the performance parameters that yields better exergy and thermal efficiency, net work produced and of course cost effective also. Moreover, optimization of the ORC was also performed with the help of response surface methodology (RSM) technique and its results revealed that at an optimized condition, R152a shows the highest value of exergy efficiency, thermal efficiency and work output among the other fluids i.e. around 98.47%, 54.72% and 141.027kJ for the desirability of 0.990.

REFERENCES

[1] P. Colonna, E. Casati, C. Trapp, T. Mathijssen, J. Larjola, T. Turunen-Saaresti, A. Uusitalo, “Organic Rankine Cycle Power Systems: From the Concept t
[2] o Current Technology, Applications, and an Outlook to the Future”, J. Eng. Gas Turb. Power, vol. 137, pp. 1-19, 2015.C. Sprouse III, C. Depcik, “Review of organic Rankine cycles for internal combustion engine exhaust waste heat recovery”, Appl. Therm. Eng., vol. 51, pp. 711–22, 2013.
[3] P. Bombarda, C.M. Invernizzi, C. Pietra, “Heat recovery from Diesel engines: A thermodynamic comparison between Kalina and ORC cycles”, Appl. Therm. Eng., vol. 30, pp. 212–9, 2010
[4] D. Di Battista, M. Mauriello, R. Cipollone, “Waste heat recovery of an ORC-based power unit in a turbocharged diesel engine propelling a light duty vehicle”, Appl. Energy, vol. 152, pp. 109–20, 2015
[5] A. Uusitalo, T. Turunen-Saaresti, J. Honkatukia, P. Colonna, J. Larjola, “Siloxanes as Working Fluids for Mini-ORC Systems Based on High-Speed Turbogenerator Technology”, J. Eng. Gas Turb. Power, Vol. 135,pp. 042305 (1–9), 2013
[6] A. Uusitalo, J. Honkatukia, T. Turunen-Saaresti, J. Larjola, “A thermodynamic analysis of waste heat recovery from reciprocating engine power plants by means of organic Rankine cycles”, Appl. Therm. Eng., vol. 70, pp. 33–41, 2014
[7] T.C. Hung, T.Y. Shai, S.K. Wang, “A review of Organic Rankine Cycles (ORCs) for the Recovery of Low-Grade Waste Heat”, Energy, vol. 22, pp. 661–667, 1997
[8] B.T. Liu, K.H. Chien, C.C. Wang, “Effect of working fluids on organic Rankine cycle for waste heat recovery,” Energy, vol. 29, pp. 1207–17, 2004
[9] H. Chen, DY Goswami, EK Stefanakos, “A review of thermodynamic cycles and working fluids for the conversion of lowgrade heat”, Renew. Sust. Energy Rev, vol. 14, pp. 3059–67, 2010
[10] P. J. Mago, “Exergetic evaluation of an organic rankine cycle using medium-grade waste heat.” Energy Sources Part A, vol. 34, pp. 1768–1780, 2012
[11] L. Wei, Y. Zhang, Y. Mu, X. Yang, X. Hu, “Simulation and experimental research of a low-grade energy conversion system using organic rankine cycles”, Energy Sources Part A, vol. 36, pp. 537–546, 2014
[12] N. F. Tumen Ozdil, M.R. Segmen, A. Tantekin, “Thermodynamic analysis of an organic rankine cycle (ORC) based on industrial data”, Applied Thermal Engineering, vol. 91, pp. 43-52, 2015
[13] G. Shu, G. Yu, H. Tian, H. Wei, X. Liang, Z. Huang, “Multi-approach evaluations of a cascade-organic rankine cycle (C-ORC) system driven by diesel engine waste heat: Part A – Thermodynamic evaluations”, Energy Conversion and Management, vol. 108, pp. 579–595, 2016
[14] M.T. Nasir, K.C. Kim, “Working fluids selection and parametric optimization of an organic rankine cycle coupled vapor compression cycle (ORC-VCC) for air conditioning using low grade heat “, Energy and Buildings, vol. 129, pp. 378–395, 2016.

[15] R. Long, Y.J. Bao, X.M. Huang, W. Liu, "Exergy analysis and working fluid selection of organic Rankine cycle for low grade waste heat recovery", Energy, vol. 73, pp. 475–483, 201
[16] V. Minea, "Power generation with orc machines using low-grade waste heat or renewable energy", Applied Thermal
[17] F. A. Al-Sulaiman, "Exergy analysis of parabolic trough solar collectors integrated with combined steam and organic rankine cycles", Energy Conversion and Management, vol. 77, pp. 441–449, 2014
[18] S. Aghahosseini, I. Dincer, "Exergoenvironmental analysis of renewable/waste heat based organic rankine cycle (orc) using different working fluids", Proceeding of global conference on global warming, Lisbon, Portugal, 2011
[19] B.F. Tchanche, G. Papadakis, G. Lambrinos, A. Frangoudakis, "Fluid selection for a low-temperature solar organic rankine cycle", Applied Thermal Engineering, vol. 29, pp. 2468–2476, 2009
[20] Q. Zhu, Z. Sun, J. Zhou, "Performance analysis of organic Rankine cycles using different working fluids," Thermal Science, vol. 19, pp. 179-191, 2015.
[21] A. Borsukiewicz-Gozdur, "Experimental investigation of R227ea applied as working fluid in the ORC power plant with hermetic turbogenerator", Applied Thermal Engineering, vol. 56, pp. 126-133, 201
[22] J. Nouman, Comparative studies and analyses of working fluids for Organic Rankine Cycles – ORC, Master of Science Thesis, KTH School of Industrial Engineering and Management, Stockholm, 2012.
[23] S. A. Klein, Engineering Equation Solver (EES), Academic Commercial V8.208, F-Chart Software, Available at: www.fChart.com, 2008.
[24] P. M. Jeganathan, S. Venkatachalam, T. Karichappan, S. Ramasamy, "Model Development and Process Optimization for Solvent Extraction of Polyphenols From Red Grapes Using Box–Behnken Design", Preparative Biochemistry & Biotechnology, vol. 44, pp. 56-67, 2014.
[25] R.H. Myers, D.C. Montgomery, Response surface methodology: Process and product optimization using designed experiments. Ist edition. John Wiley and Sons, New York, 2002; ISBN: 0471412554
[26] D.Y. Goswami, http://www.iitj.ac.in/CSP/material/19dec/thermodynamic.pdf (accessed on 21/5/2017)

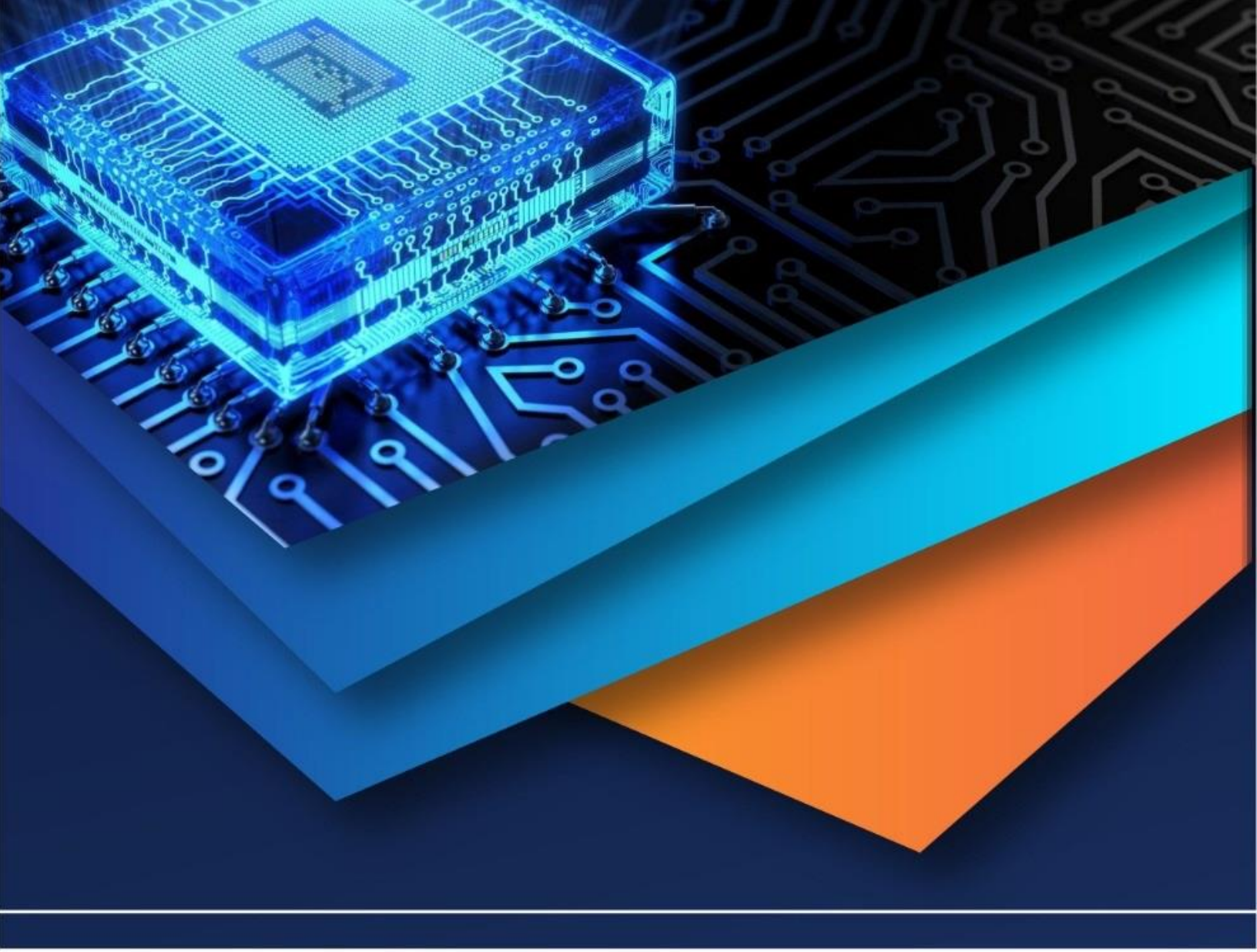

10.22214/IJRASET

45.98

IMPACT FACTOR: 7.129

IMPACT FACTOR: 7.429

INTERNATIONAL JOURNAL FOR RESEARCH

IN APPLIED SCIENCE & ENGINEERING TECHNOLOGY